

## Multichannel multislice B1+ mapping

In this study, multichannel multislice B1+ maps were obtained by using a hybrid method, which combines a single large tip angle AFI together with a series of small tip angle gradient echo images. Relevant imaging parameters for the AFI were: FOV=320(RO)×216(PE)×176.4(SS) mm<sup>3</sup> (where RO, PE and SS designate readout, phase encode and slice selective dimensions, respectively), in-plane resolution= 4 mm, slice thickness=6.3 mm, TR1/TR2/TE=20/100/2.13 ms, nominal flip angle=60°, in-plane acceleration factor=2 (i.e., iPAT=2 in Siemens terminology), partial Fourier=6/8 (PE and SS), bandwidth=320 Hz/pixel and total acquisition time=3 minutes 11 seconds. The series of small tip angle gradient echo images were acquired with the relevant imaging parameters being FOV=320(RO)×216(PE) mm<sup>2</sup>, in-plane resolution=4 mm, 24 sagittal slices, slice thickness=6.3 mm, TR/TE=250/2.76 ms, nominal flip angle=10°, iPAT=2, partial Fourier=7/8 (PE), bandwidth=380 Hz/pixel and total acquisition time=1 minute 30 seconds.

## T1 weighted 3D-MPRAGE acquisition

The T1-weighted image obtained for masking the brain was acquired using the MPRAGE sequence (1) with the following imaging parameters: FOV=224(RO)×224(PE) ×179.2(SS) mm<sup>3</sup>, 0.7-mm isotropic resolutions, TR/TE/TI=2400/2.68/1300 ms, nominal flip angle=6°, iPAT=2, partial Fourier=7/8 (PE), phase oversampling=10%, bandwidth=210 Hz/pixel and total acquisition time=6 minutes 36 seconds. To reduce the impact of B<sub>1</sub><sup>+</sup> inhomogeneity on inversion, adiabatic pulses (2) using the phases obtained from the CP-like mode RF phase shimming were utilized.

## Pilot high resolution dMRI with 2-fold slice acceleration

Using each of the three transmit configurations under consideration, we acquired the 1.05-mm, single-shell, whole brain dMRI data with: FOV=210(RO)×210(PE) ×151.2(SS) mm<sup>3</sup>, anterior-posterior phase encoding, MB2, inter-slice shift=FOV/2, iPAT=3, partial Fourier=6/8, 144 sagittal slices, TR/TE=7400/71 ms, bandwidth=1388 Hz/pixel, and echo spacing=0.82 ms.

1  
2  
3 As in the 7T HCP dMRI protocol, excitation and refocusing MB pulses were formed using  
4 vendor optimized apodized sinc pulses with TBWP=3.2 for excitation, and TBWP=5.2 for  
5 refocusing. The pulse duration was set to 5120  $\mu\text{s}$  for excitation and 10240  $\mu\text{s}$  for refocusing.  
6  
7 Furthermore, a time shift of 1920  $\mu\text{s}$  was introduced between the two SB pulse components of  
8 the final MB2 pulses (3), as in the 7T HCP dMRI data (4), leading to total pulse duration of 7040  
9  $\mu\text{s}$  for excitation and 12160  $\mu\text{s}$  for refocusing.  
10  
11

12  
13 The pTx dMRI dataset was acquired with the pTx-enabled sequence, whereas the two 1Tx  
14 dMRI datasets were obtained with the sequence that had been used in the WashU-Minn-Oxford  
15 consortium of the HCP (4). For the pTx acquisition, the RF voltages were adjusted to achieve  
16 the nominal flip angles (i.e., 90° for excitation and 180° for refocusing) at the maximum  $B_1^+$  field  
17 across the brain. For 1Tx acquisitions, because of the more inhomogeneous RF field across the  
18 brain, relatively higher reference RF voltages (set to achieve 10-15% greater than nominal flip  
19 angles) were utilized to increase the signals from the low  $B_1^+$  regions in the periphery of the  
20 brain.  
21  
22

23  
24 For the pTx dMRI acquisition, the same 24 RF shim sets were utilized for both excitation and  
25 refocusing. These RF shim sets were utilized to form 12 pairs of band-specific or slab-specific  
26 pTx excitation and refocusing MB2 pulses (a total of 48 pTx MB2 pulses). During data  
27 acquisition, each pair was applied six times with adjusted central frequencies to excite and  
28 refocus the 12, 1.05-mm thick image slices residing within the two corresponding 6.3-mm thick  
29  $B_1^+$  mapping slabs (each with 6 image slices), leading to the acquisition of a total of 144 image  
30 slices per image volume.  
31  
32  
33  
34  
35  
36  
37  
38  
39

## 40 **Original HCP 7T diffusion protocol**

41  
42  
43 The HCP 7T diffusion protocol acquires whole brain dMRI data with 1.05 mm isotropic  
44 resolutions, FOV=210(RO)  $\times$  210(PE)  $\times$  138.6(SS) mm<sup>3</sup>, MB2, iPAT=3 (3-fold in-plane  
45 acceleration), partial Fourier=6/8, inter-slice shift=FOV/2, 132 oblique axial slices,  
46 TR/TE=7000/71 ms, bandwidth=1388 Hz/pixel, echo spacing=0.82 ms, and two-shell q-space  
47 sampling (b-value=1000 and 2000 s/mm<sup>2</sup>); it acquires a total of 286 image volumes,  
48 corresponding to 64 unique diffusion directions per shell plus 15 interspersed b=0 images,  
49 acquired twice using anterior-posterior (AP) and PA phase encode directions. The total  
50 acquisition time was ~40 minutes, which was divided into 4 segments of ~10 minutes each (the  
51 reader is referred to Vu et al. (4) for more details on the HCP 7T dMRI protocol).  
52  
53  
54  
55  
56  
57  
58  
59  
60

## Supporting Figures

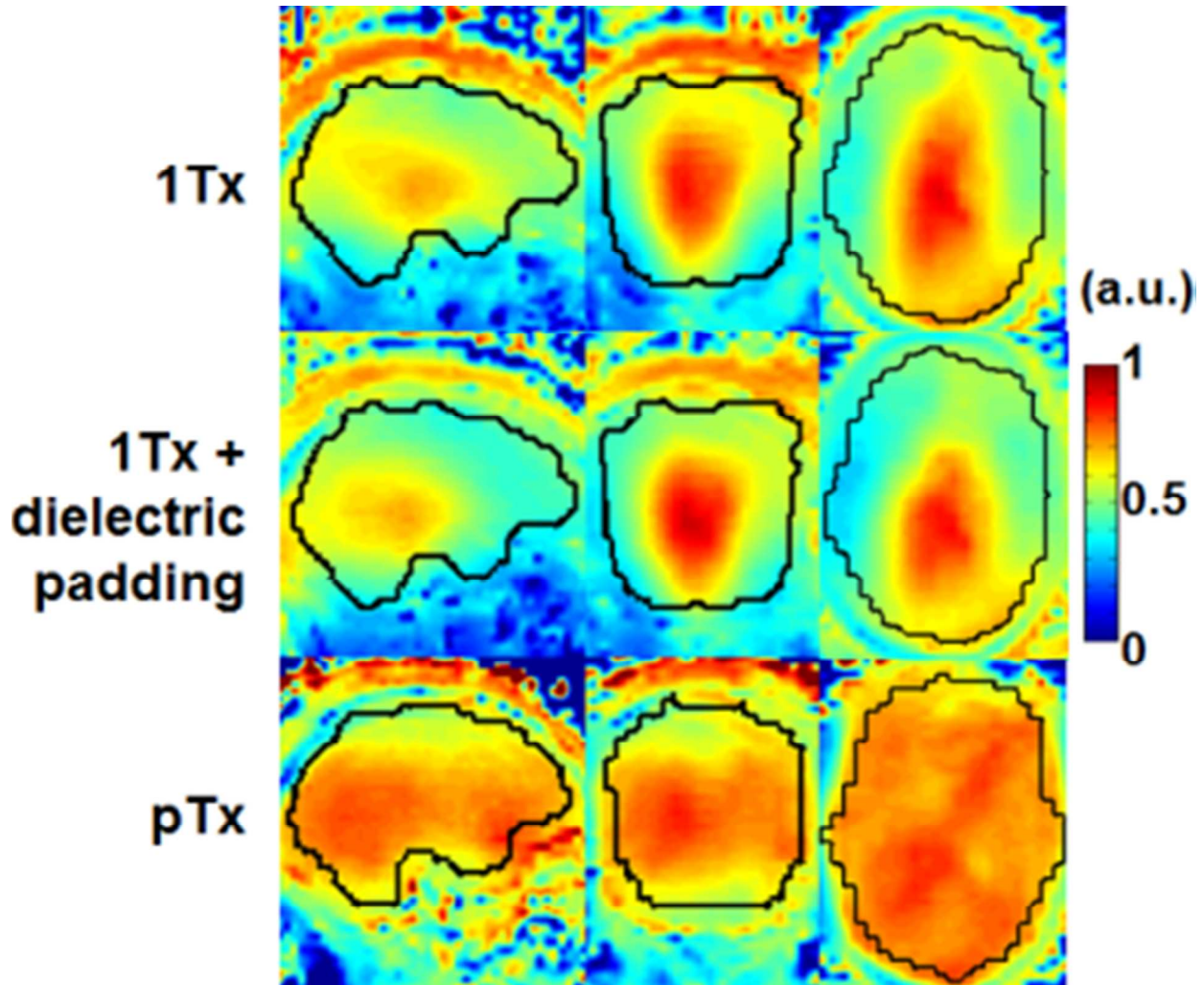


Fig. S1. Magnitude transmit B1 ( $B1+$ ) maps for Nova single transmit (1Tx) coil alone (top row) and with dielectric padding (middle row), Nova 8 transmit (8Tx) coil with pTx multiband (MB) pulse design (bottom row).  $B1+$  maps are shown in three orthogonal views with brain regions indicated by black curves. Following the slab-wise design framework, band-specific RF shimming was conducted on 24 contiguous, 6.3-mm thick sagittal  $B1+$  mapping slabs covering the whole brain. The brain mask utilized was derived by extracting the brain from a 3D T1w image acquired with 0.7 mm isotropic resolutions. Note that pTx yielded best  $B1+$  homogeneity across the whole brain.

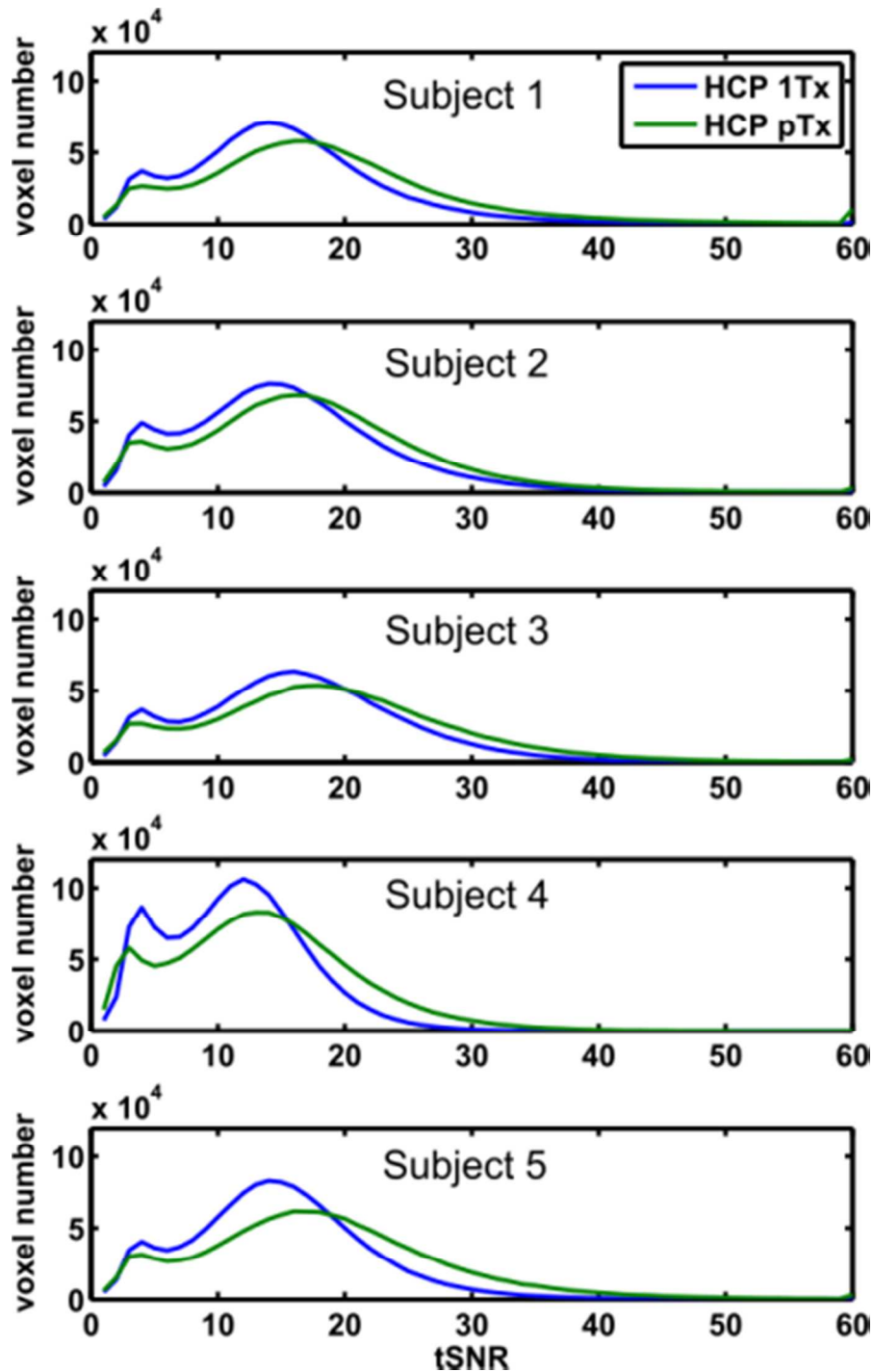
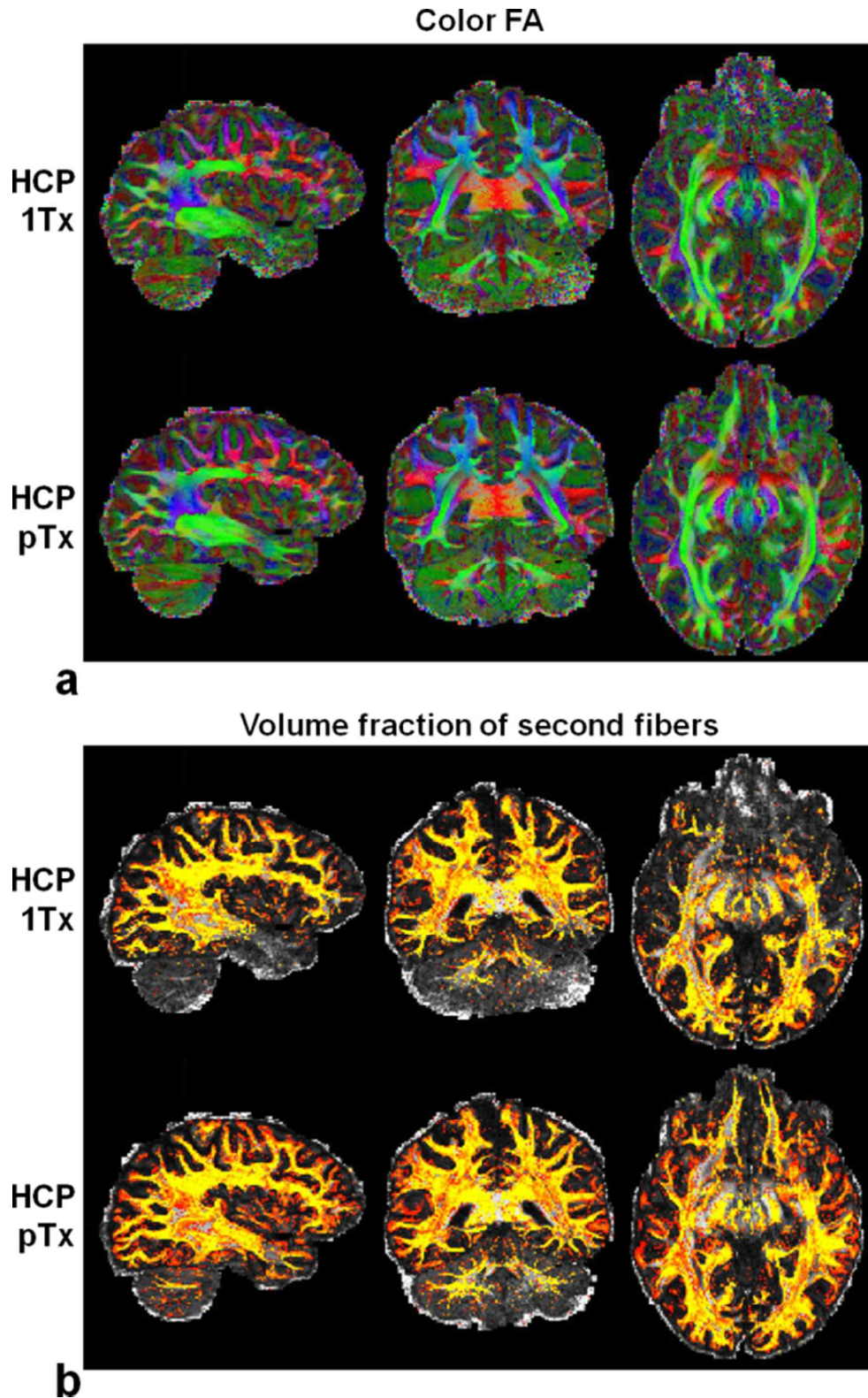


Fig. S2. Comparing HCP 7T dMRI protocol (HCP 1Tx) with HCP pTx protocol in terms of histograms of temporal SNR (tSNR). Each row shows tSNR histograms for one subject. For each subject, the tSNR histogram for HCP 1Tx (blue) or HCP pTx (green) dataset was created by counting the voxels in the brain mask and based on the tSNR map that were calculated on a voxel-wise basis from the corresponding 15, minimally preprocessed, b0 images obtained at different time points during the dMRI acquisition. Further quantitative analysis revealed that the use of pTx on average increased tSNR in ~63% of the brain volume.



53 Fig. S3. Comparing HCP 7T dMRI protocol (HCP 1Tx) with HCP pTx protocol. Data are shown  
54 for another subject. (a) Color fractional anisotropy (FA) maps. (b) Volume fraction maps for  
55 second fiber orientations. The color FA is FA (in the range of [0 1]) with the color representing  
56  
57  
58  
59  
60

1  
2  
3 the orientation of the principal fiber (red: left-right; green: anterior-posterior; blue: inferior-  
4 superior). The volume fraction map is shown in a colorscale of [0.05 0.2] (with yellow being high  
5 and red being low in volume fraction), overlaid on the respective FA map (in a grayscale of [0 1]).  
6 Both dMRI datasets were acquired with 1.05 mm isotropic resolutions, MB2, in-plane  
7 acceleration factor=3, and TE=71 ms. The TR for pTx acquisition was slightly longer (7400 vs  
8 7000 ms). Both acquisitions utilized the same q-space sampling scheme (double shells, b-  
9 value=1000/2000 s/mm<sup>2</sup>), corresponding to 143 unique image volumes, each acquired twice  
10 with anterior-posterior (AP) and PA phase encode directions. Total scan time was kept constant  
11 for both datasets (i.e., 40 minutes divided into 4 segments of 10 minutes each). Note that the  
12 use of pTx improved fiber orientation estimation performances in such brain regions as the  
13 lower temporal lobe, the cerebellum and the inferior frontal lobe.  
14  
15  
16  
17  
18  
19  
20  
21  
22  
23  
24  
25  
26  
27  
28  
29  
30  
31  
32  
33  
34  
35  
36  
37  
38  
39  
40  
41  
42  
43  
44  
45  
46  
47  
48  
49  
50  
51  
52  
53  
54  
55  
56  
57  
58  
59  
60

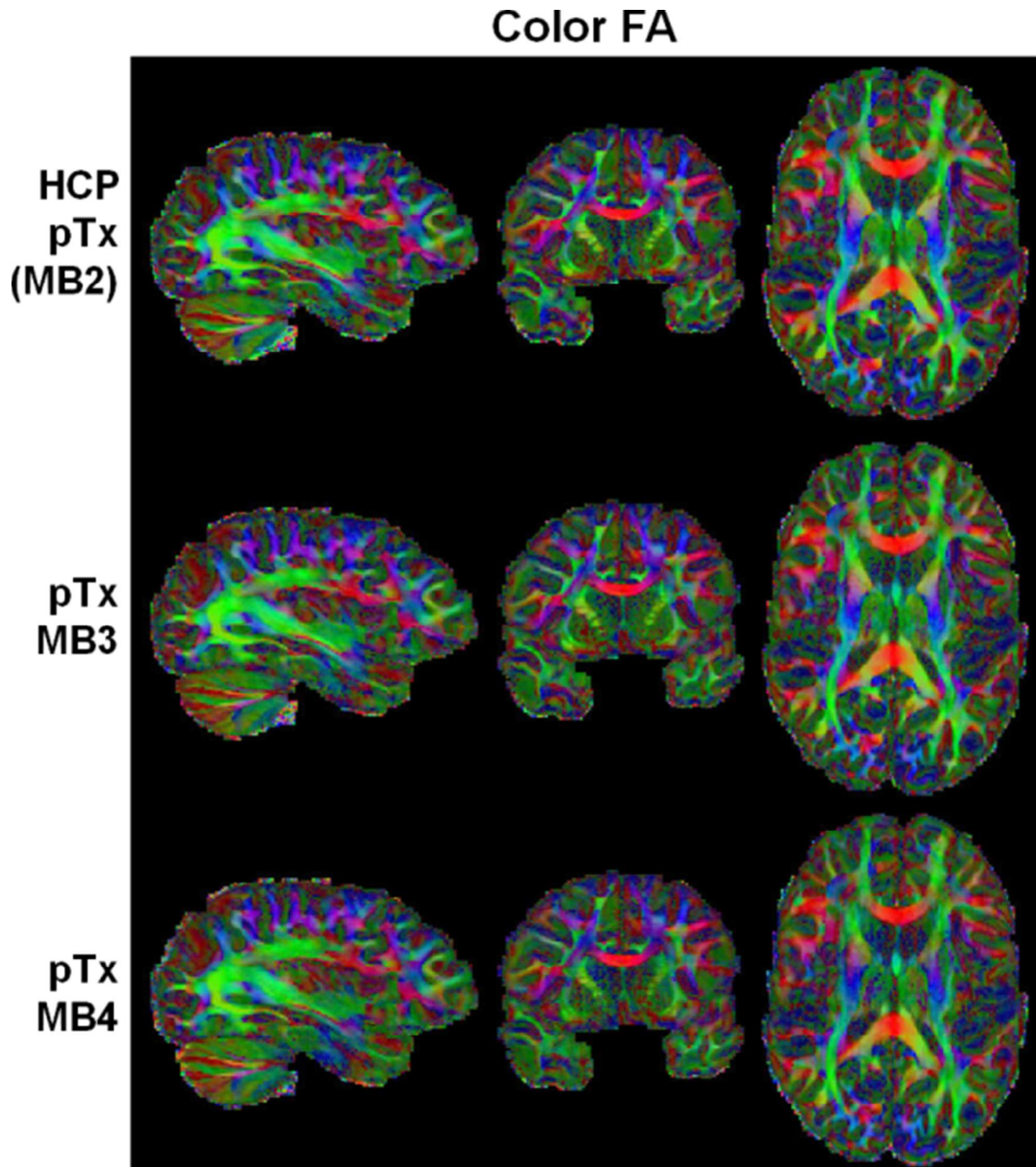
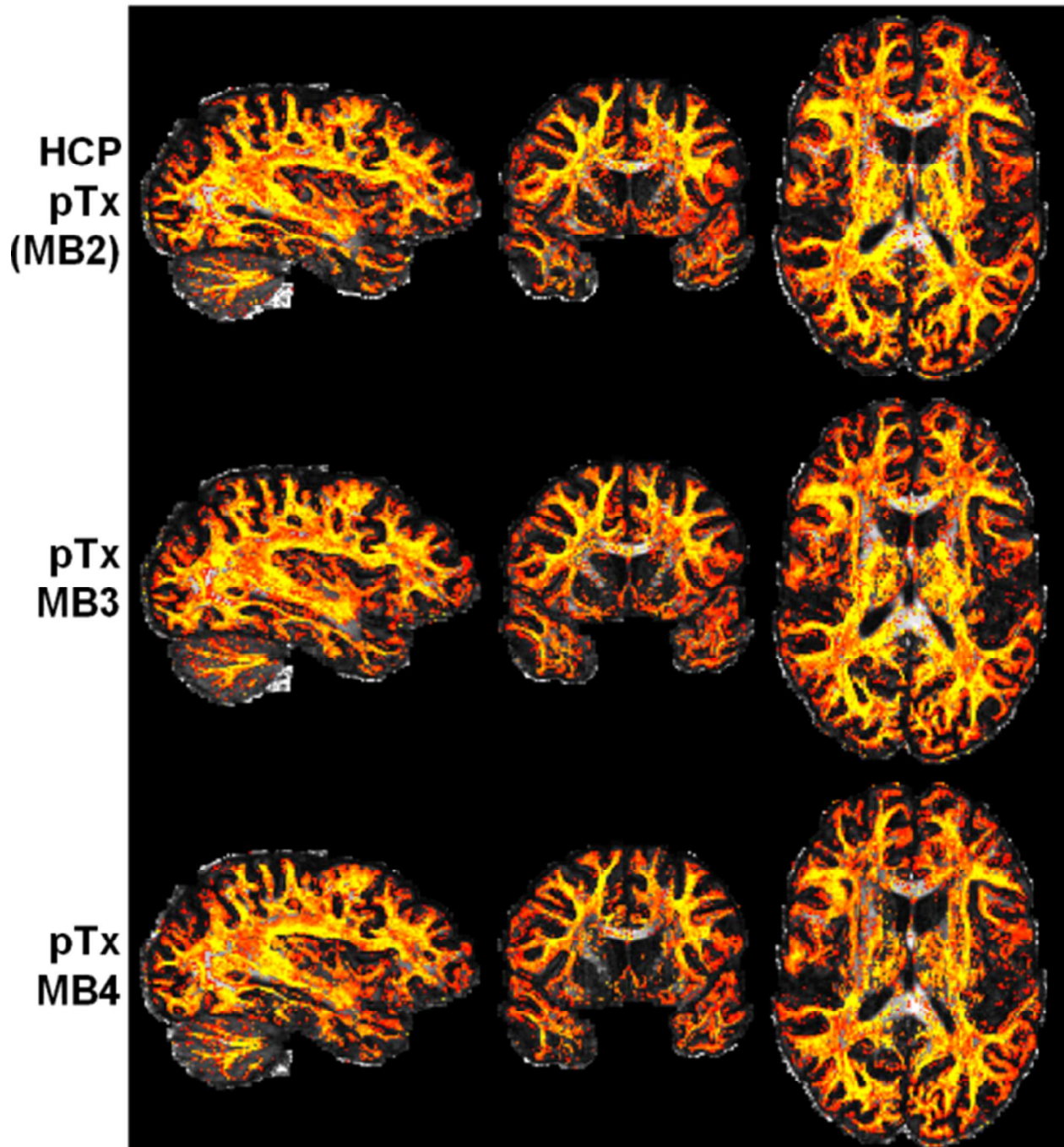


Fig. S4. Color fractional anisotropy (FA) maps of the HCP pTx MB2 protocol (top row) vs the pTx MB3 protocol (middle row) vs the pTx MB4 protocol (bottom row) in another subject. The color FA is FA (in the range of [0 1]) with the color representing the orientation of the principal fiber (red: left-right; green: anterior-posterior; blue: inferior-superior). All three dMRI datasets were acquired with 1.05 mm isotropic resolutions, in-plane acceleration factor=3, TE=71 ms, and double-shell q-space sampling (b-value=1000/2000 s/mm<sup>2</sup>). Total scan time was kept constant for all acquisitions (i.e., ~40 minutes divided into 4 segments of 10 minutes each).

1  
2  
3 Because of use of a shorter TR (3701 ms for MB4 and 4934 ms for MB3 vs 7400 ms for MB2),  
4 both MB3 and MB4 acquisitions obtained more data than the MB2 acquisition.  
5  
6  
7

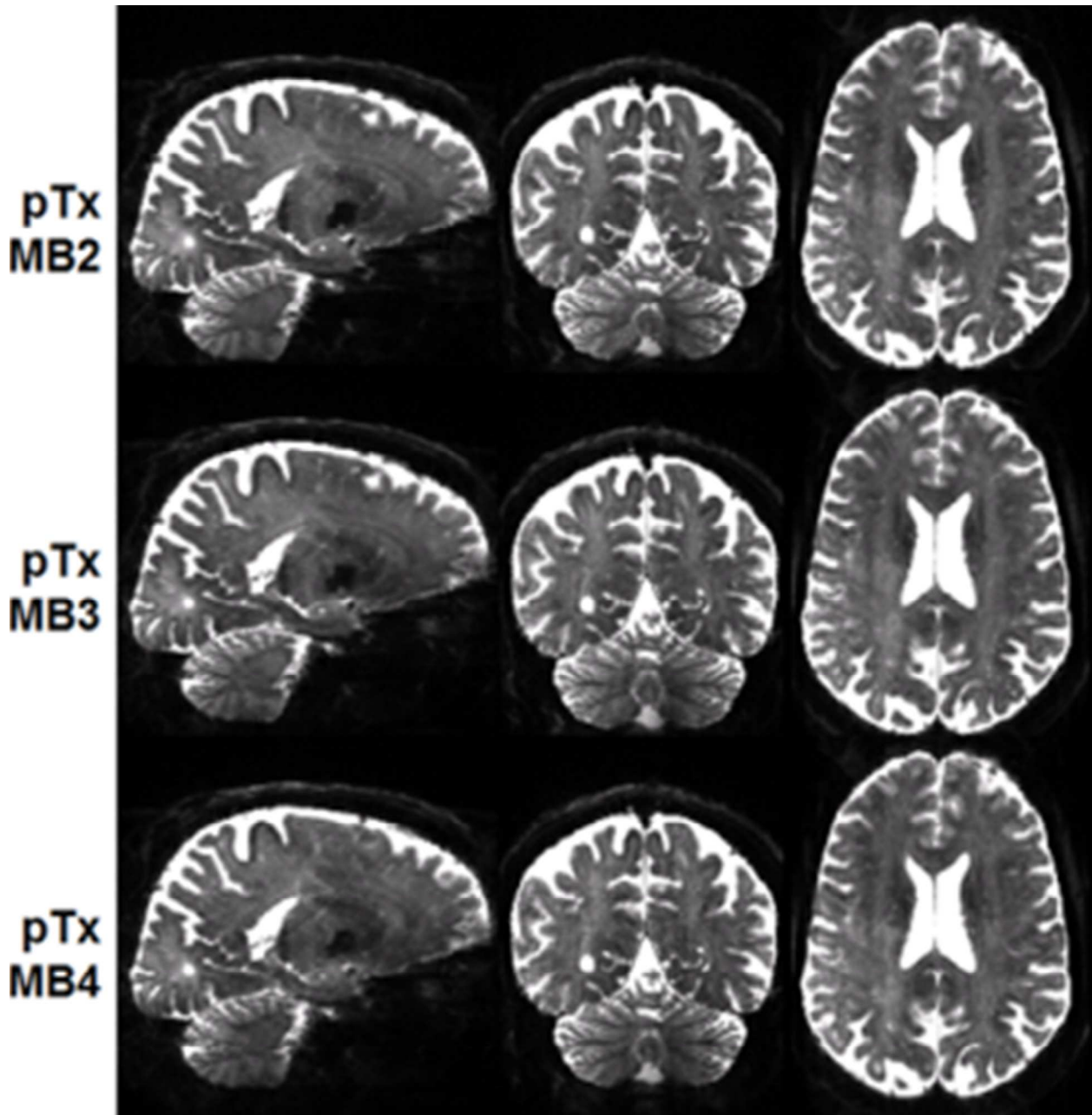
## 8 Volume fraction of second fibers



54 Fig. S5. Volume fraction maps of second fiber estimation for the HCP pTx MB2 protocol (top  
55 row) vs the pTx MB3 protocol (middle row) vs the pTx MB4 protocol (bottom row) in another  
56  
57  
58  
59  
60



1  
2  
3 subject. These volume fraction maps derived using the same data as in Fig. S4, are overlaid on  
4 the respective fractional anisotropy map (defined in the grayscale of [0 1]) and shown in a  
5 colorscale of [0.05 0.2] (with yellow being high and red being low in volume fraction).  
6  
7  
8  
9

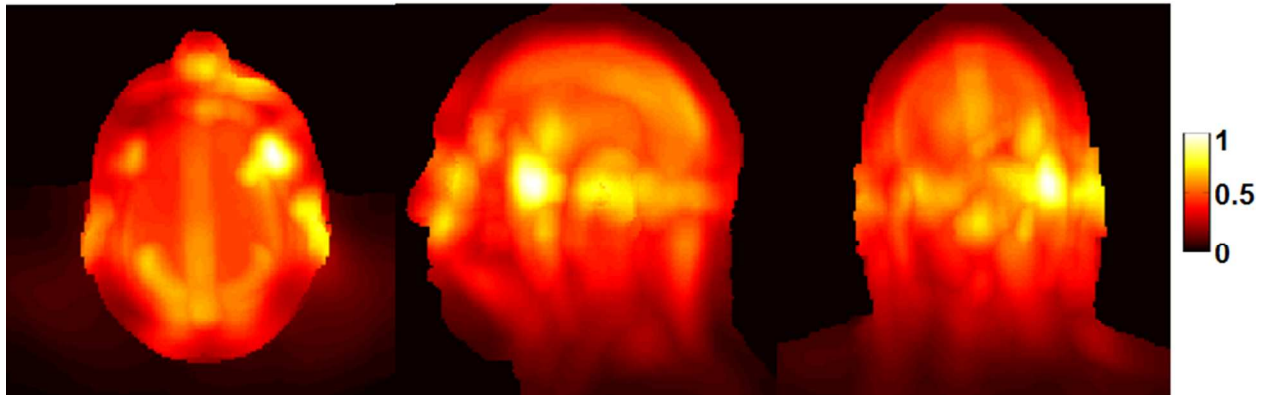


50  
51 Fig. S6. Comparison of image quality for pTx acquisition with MB2 vs MB3 vs MB4, all with an  
52 in-plane acceleration of 3 (iPAT3). Shown are distortion corrected  $b=0$  images acquired with  
53 1.05 mm isotropic resolutions. Although enabling shorter TR values, both MB3 and MB4 data  
54 acquisitions used the same TR of 7400 ms as MB2 acquisition to avoid the TR dependent signal  
55 saturation effect for comparison purposes. All images were reconstructed using the split slice-  
56  
57  
58  
59  
60

1  
2  
3 GRAPPA algorithm (Cauley et al. MRM 2014) to minimize the inter-band signal leakage. Note  
4 that both MB3 and MB4 acquisitions led to comparable image quality to the MB2 acquisition.  
5  
6  
7

### 8 **Maximum intensity projection of 10-g SAR**

9



23  
24 Fig. S7. Maximum intensity projection of the local SAR distribution in axial (left), sagittal (middle)  
25 and coronal (right) view for the pTx multiband pulses utilized in the current study. The local SAR  
26 map shown here is normalized to the maximum, mainly to appreciate the location of the  
27 hotspots. Note the SAR hotspots observed in various regions of the head. This same  
28 normalized local SAR distribution applies to all of the pTx dMRI acquisitions in the current study,  
29 but the absolute value for the maximum local SAR varies, depending on what MB factor is used  
30 for the acquisition. The maximum local SAR value was calculated to be 0.95, 1.42 and 1.70  
31 W/kg for MB2, MB3 and MB4, respectively.  
32  
33  
34  
35  
36  
37  
38  
39  
40  
41  
42  
43  
44  
45  
46  
47  
48  
49  
50  
51  
52  
53  
54  
55  
56  
57  
58  
59  
60

## References

1. Mugler JP, 3rd, Brookeman JR. Three-dimensional magnetization-prepared rapid gradient-echo imaging (3D MP RAGE). *Magn Reson Med* 1990;15(1):152-157.
2. Garwood M, DelaBarre L. The return of the frequency sweep: designing adiabatic pulses for contemporary NMR. *Journal of magnetic resonance (San Diego, Calif: 1997)* 2001;153(2):155-177.
3. Auerbach EJ, Xu J, Yacoub E, Moeller S, Ugurbil K. Multiband accelerated spin-echo echo planar imaging with reduced peak RF power using time-shifted RF pulses. *Magn Reson Med* 2013;69(5):1261-1267.
4. Vu AT, Auerbach E, Lenglet C, Moeller S, Sotiropoulos SN, Jbabdi S, Andersson J, Yacoub E, Ugurbil K. High resolution whole brain diffusion imaging at 7T for the Human Connectome Project. *NeuroImage* 2015;122:318-331.